Human-like control strategy of a bipedal walking model

Andrej Olenšek* and Zlatko Matjačić

Institute for Rehabilitation, Republic of Slovenia, Linhartova 51, SI-1000 Ljubljana, Slovenia.

SUMMARY

This paper presents a two-level control strategy for bipedal walking mechanism that accounts for implicit control of push-off on the between-step control level and tracking of imposed holonomic constraints on kinematic variables via feedback control on within-step control level. The proposed control strategy was tested in a biologically inspired model with minimal set of segments that allows evolution of human-like push-off and power absorption. We investigated controller's stability characteristics by using Poincaré return map analysis in eight simulation cases and further evaluated the performance of the biped walking model in terms of how variations in torso position and gait velocity relate to push-off and power absorption. The results show that the proposed control strategy, with the same set of controller's gains, enables stable walking in a variety of chosen gait parameters and can accommodate to various trunk inclinations and gait velocities in a similar way as seen in humans.

KEYWORDS: Push-off; Power absorption; Feedback control; Within-step control; Between-step control.

1. Introduction

Even though biomechanics of human locomotion is well understood[1,2] and human walk appears plain, we have been confronted with many difficulties when attempting to mimic human walking in bipedal robots as we do not yet have a full understanding of control principles that underlie body support and forward propulsion in legged locomotion. This has motivated rapid progress in design of numerous biped walking models[3–10] and robots[11–17] that allow us to examine various control strategies.

The simplest bipedal machines are passive dynamic[9,12,13,17,18] and ballistic[11,15,19] walking models that have only few degrees of freedom. Passive dynamic walking models are free from actuation and utilize inertial and gravitational forces to develop stable walking down the slope. A similar principle is applied in ballistic walking, where the swing leg is actuated only at the beginning and the end of the stance phase, with the inertial and gravitational forces being utilized elsewhere. This class of bipedal mechanisms is energy efficient, and generates stable limit cycles that fully determine kinematics and require little effort to control

but simultaneously lack the robustness and insensitivity to disturbances making them of little practical use.

More sophisticated bipedal robots with many actuated degrees of freedom follow trajectories that are predetermined either through human gait analyses constructed templates[7,8] or calculated through optimization of certain cost criteria,[6,20,21] while the stability is achieved by the zero-moment point (ZMP) control.[15,22,23] While such an approach enables practical locomotion, the requirement for *a priori* determination of specific kinematics imposes significant limitations on the versatility of such bipedal machines.

An approach that does not require specification of trajectories in advance was provided by Grizzle *et al.*[3,5] who proposed a feedback control of a set of scalar-valued functions of the states of the robot. These scalar-valued functions encode certain walking premises like keeping the trunk upright and symmetrical movement of both legs. Grizzle *et al.*[5] have developed a five degrees of freedom model, where all scalar-valued functions are expressed as a function of the stance leg inclination, which enables derivation of a formal proof of asymptotic stability of the derived controller for certain model parameters. The model assumes some standard simplifications, the most important being the instantaneous transition from the single support to a swing phase. This simplification presents a serious limitation for control of bipedal machines, because lack of a double support phase means that restitution of lost energy at the impact of swinging leg with the ground cannot be accomplished in a similar way as in human locomotion. Analysis of human walking shows that the majority of power generation occurs at the end of stance phase when a forceful extension of the trailing leg also termed as a push-off takes place, followed by an eccentric flexion of the leading leg performing majority of power absorption within the double support phase.[24–26] Incorporating such human-like behavior into control of bipedal walking model represents a considerable challenge and has not been extensively addressed. There have been attempts where the energy dissipated during contact was replaced by applying force impulses to the stance leg just before heel strike.[24,27] However, this was done on the assumption that the time duration of the impulses was instantaneous, which is not practical for application in real mechanisms. Miossec *et al.*[28] presented a model that included a finite time-duration double support in a gait cycle but without preceding push-off.

In this paper, we propose a novel control strategy that implicitly incorporates control of a push-off of the trailing leg in the second half of the singles-stance phase and succeeding

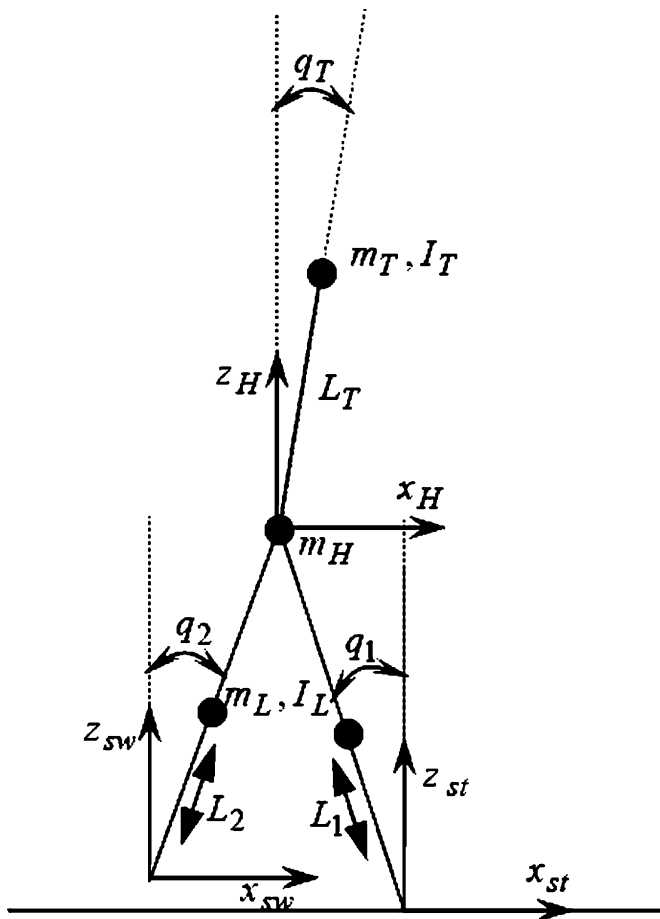* Corresponding author. E-mail: andrej.olensek@ir-rs.si

Fig. 1. Schematic representation of the biped model.

power absorption of the leading leg within the double support phase. This is achieved by a combination of the standard feedback control principles throughout the gait cycle and adaptive variation of the desired leg length at the end of each cycle resulting in a time-variant zero dynamics. The controller's stability is evaluated in simulations by the use of Poincaré return map analysis and the performance of the biped walking model in different walking modes is qualitatively compared to human walking in terms of ground reaction forces.

2. Robot Model and Modeling Assumptions
The modeling approach presented in this paper is closely related to the work of Grizzle *et al.*[3,5] The robot is considered bipedal and planar with five degrees of freedom. It is assumed to have two telescopic legs that are connected at hip by ideal revolute joints and are carrying the torso segment. There is a mass at the center of each leg and two masses at the hips and the end of a torso segment, respectively. Finally a force actuator is applied at each leg and two torques between the torso and each leg, but not at the contact point of the leg with the ground. We consider the described model as a minimal configuration that is capable of mimicking human locomotion and reproducing human-like walking patterns in terms of ground reaction forces. A representative model structure is shown in Fig. 1.

We will adopt identical division of gait cycle as in human walking. A complete human gait cycle may be divided into phases of single support (one leg in contact with the ground) and double support (both legs in contact with the ground). The leg that throughout the single support phase remains in contact with the ground will be referred to as the stance leg. Likewise, the leg that in single support phase advances toward the point of the next contact will be referred to as the swing leg. When both legs remain in contact with the ground during the double support, the legs will be referred to according to their function in the preceding single support phase, thus stance and swing leg.

The transition from the single support to double support phase is referred to as the contact phase and is associated with the swing leg touching the ground. Likewise, the transition from double support to single support phase is referred to as the take-off phase and is associated with the rear leg lifting of the ground. Both transition phases are assumed to be instantaneous. The dynamic equations are composed of ordinary differential equations for the support phases and algebraic equations for the transition phases.

2.1. Single support phase
Let $q = (q_1, q_2, q_T, L_1, L_2, x_H, z_H)^T$ be the set of coordinates describing the configuration of the robot with respect to a world reference frame and $u = (T_1, T_2, F_1, F_2)^T$ the torques between the torso and each leg and forces in each leg respectively, as shown in Fig. 1. To account for switching between the single and double support phases, we will further denote $q_{st} = q_1$, $q_{sw} = q_2$, $L_{st} = L_1$, $L_{sw} = L_2$, $T_{st} = T_1$, $T_{sw} = T_2$, $F_{st} = F_1$, and $F_{sw} = F_2$, when legs one and two are considered as stance and swing leg, respectively, in a current single support and succeeding double support phase. Likewise, we will denote $q_{st} = q_2$, $q_{sw} = q_1$, $L_{st} = L_2$, $L_{sw} = L_1$, $T_{st} = T_2$, $T_{sw} = T_1$, $F_{st} = F_2$, and $F_{sw} = F_1$, when legs one and two are considered as swing and stance leg, respectively, in a current single support and succeeding double support phase.

The stance leg contacting the ground throughout the single support phase adds two supplementary constraints in the form $x_{st} = \text{const}$, $z_{st} = 0$, thereby reducing the feasible space of motion to a constraint surface. The constraints are organized in matrix form as $\Psi_{ss}(q) = 0$ and introduced into dynamic equations via Lagrange multipliers. Hence, forming the Euler–Lagrange equations of the constrained system, the model is written in the form

$$M(q)\ddot{q} + C(q, \dot{q})\dot{q} + G(q) = Bu + \Gamma_{ss}^T \lambda_{ss}$$
$$T_{ss,start} < t < T_{ss,end} \quad (1)$$
$$\Gamma_{ss}\dot{q} = \frac{\partial \Psi_{ss}}{\partial q}\dot{q} = 0$$

where $M(q)$ is the inertia matrix, $C(q, \dot{q})$ is the matrix of centripetal and Coriolis terms, $G(q)$ is the gravity vector, and λ_{ss} is a vector of Lagrange multipliers equal to negative ground reaction forces during single support. $T_{ss,start}$ and $T_{ss,end}$ denote the times of the start and end of single support phase, respectively. The model is written in the state space

form by

$$\dot{x}_{ss} = \begin{bmatrix} \dot{q} \\ M^{-1}(q)\big[-C(q,\dot{q})\dot{q} - G(q) + Bu + \Gamma_{ss}^T\lambda_{ss}\big] \end{bmatrix}$$

$$=: f_{ss}(x_{ss}) + g_{ss}(x_{ss})u. \tag{2}$$

2.2. Contact phase

A standard rigid contact model is assumed.[29] Basic hypotheses of the contact model are:

- The impact is inelastic and without slipping.
- The impact is instantaneous.
- The external forces during the impact can be represented by impulses and cannot be generated by actuators
- The impulse forces may result in velocity but not position discontinuities.

Hence, the angular momentum is conserved, leading to

$$M(\dot{q}^+ - \dot{q}^-) = F_{c,ext} \tag{3}$$

where $\dot{q}^+$ and $\dot{q}^-$ are velocity vectors just before and just after the impact, respectively, and $F_{c,ext}$ the contact impulse forces.

Four constraint equations in the form $x_{st} = const_1$, $z_{st} = 0$, $x_{sw} = const_2$, and $z_{sw} = 0$ completely characterize the contacts of both legs with the ground after the impact and are organized in matrix form $\Psi_c(q) = 0$. The following relation determines the admissible set of velocities after the impact:

$$\Gamma_c\dot{q}^+ = \frac{\partial\Psi_c}{\partial q}\dot{q}^+ = 0. \tag{4}$$

With an additional equation relating the impulse during contact $F_{c,ext}$ to the tangent and normal forces during contact F_c at the tips of both legs

$$F_{c,ext} = \Gamma_c^T(q_c)[F_{T1} \ \ F_{N1} \ \ F_{T2} \ \ F_{N2}]^T = \Gamma_c^T(q_c)F_c, \tag{5}$$

the following set of equations is solved for joint velocities just after the impact $\dot{q}^+$

$$\begin{bmatrix} M & -\Gamma_c^T \\ \Gamma_c & 0 \end{bmatrix} \cdot \begin{bmatrix} \dot{q}^+ \\ F_c \end{bmatrix} = \begin{bmatrix} M\dot{q}^- \\ 0 \end{bmatrix} \quad t = T_c = T_{ss,end} = T_{ds,start} \tag{6}$$

where T_c denotes the contact time and Eq. (6) illustrates the instantaneous transition to double support.

Geometrically, the contact model can also be considered as an $M(q)$-orthogonal projection of $\dot{q}^-$ onto the feasible space $\{\dot{q}^+ \in T_qQ | \Gamma_c\dot{q}^+ = 0\}$,[9] i.e., a mapping from higher-dimensional space of single support to a lower-dimensional constraint surface of double support, hence resulting in velocity discontinuities.

2.3. Double support phase

Both legs in contact with the ground throughout the double support phase introduce four constraint equations, thereby reducing the feasible space of motion to a constraint surface.

They are identical, as in previous section; however, for consistency reasons, they are expressed as $x_{st} = const_1$, $z_{st} = 0$, $x_{sw} = const_2$, $z_{sw} = 0$ or in matrix form $\Psi_{ds}(q) = 0$ and introduced into dynamic equations via Lagrange multipliers

$$M(q)\ddot{q} + C(q,\dot{q})\dot{q} + G(q) = Bu + \Gamma_{ds}^T\lambda_{ds}$$

$$\Gamma_{ds}\dot{q} = \frac{\partial\Psi_{ds}}{\partial q}\dot{q} = 0$$

$$T_{ds,start} < t < T_{ds,end} \tag{7}$$

where λ_{ds} is a vector of Lagrange multipliers equal to negative ground reaction forces during double support. $T_{ds,start}$ and $T_{ds,end}$ denote the times of the start and end of double support phase, respectively. The model is written in the state space form

$$\dot{x}_{ds} = \begin{bmatrix} \dot{q} \\ M^{-1}(q)\big[-C(q,\dot{q})\dot{q} - G(q) + Bu + \Gamma_{ds}^T\lambda_{ds}\big] \end{bmatrix}$$

$$=: f_{ds}(x_{ds}) + g_{ds}(x_{ds})u. \tag{8}$$

2.4. Take-off phase

Considering that only one leg remains in contact with the ground in succeeding single support phase, the take-off phase transition model has to account for two constraint equations in the form $x_{st} = const$, $y_{st} = 0$ or organized in matrix form $\Psi_{top}(q) = 0$. Hence, by adjusting the transition model of the contact phase in this sense, the model can be rewritten to obtain the transition model of the take-off phase, thus expressing the relation between velocities just before and just after the take-off

$$\begin{bmatrix} M & -\Gamma_{top}^T \\ \Gamma_{top} & 0 \end{bmatrix} \cdot \begin{bmatrix} \dot{q}^+ \\ F_{top} \end{bmatrix} = \begin{bmatrix} M\dot{q}^- \\ 0 \end{bmatrix}$$

$$t = T_{top} = T_{ds,end} = T_{ss,start} \tag{9}$$

where $\Gamma_{top} = \frac{\partial\Psi_{top}}{\partial q}$, $\dot{q}^+$ and $\dot{q}^-$ are velocities just after and just before the take-off, respectively, F_{top} represents tangent and normal forces at the tip of the leg, which remains in contact with the ground in succeeding single support phase, T_{top} denotes the contact time, and Eq. (9) illustrates instantaneous transition to single support phase.

Geometrically, the transition model of the take-off phase may also be considered as an $M(q)$-orthogonal projection of $\dot{q}^-$ onto the feasible space $\{\dot{q}^+\epsilon T_q|\Gamma_{top}\dot{q}^+ = 0\}$.[9] It is a mapping from lower-dimensional constrained space of double support to a higher-dimensional space of single support and solving (9) for $\dot{q}^+$, therefore, resulting in no velocity discontinuities.

3. Control Strategy

This section develops a two-level control strategy that accounts for explicit trajectory tracking via feedback control on lower level and implicit control of propulsion, push-off, and power absorption on a higher level. On lower level, we adopt similar control principle as presented by Grizzle *et al.*,[3,5] i.e., to encode walking mechanisms in postural terms that are expressed as a set of holonomic constraints

of the kinematic variables and as outputs of a mechanical model imposed on the robot via feedback control, henceforth within-step control. Our proposal is to adaptively modify these constraints after each gait cycle on higher, between-step, control level in such a manner as to adjust forward propulsion to achieve desired gait velocity and step-length control. Within-step control further comprises a feedback control in single support phase and a combination of forward dynamics and feedback control in double support phase. As both transition phases are assumed instantaneous, no control is applied neither during contact nor during take-off phase.

3.1. Within-step control

3.1.1. Within-step control in single support phase. In human walking, one observes that the torso is maintained at a nearly vertical position, the swing leg behaves roughly as a mirror image of the stance leg, the vertical hip movement is minimized, and sufficient foot clearance is assured during the swing phase. These observations have been used to build a set of control objectives in the form of the following output functions:

$$
\begin{aligned}
y_1 &= q_T - r_1 \\
y_2 &= q_{st} + q_{sw} - r_2 \\
y_3 &= z_{sw} - r_3 \\
y_4 &= L_{st} - r_4
\end{aligned}
\tag{10}
$$

where $r_i, i = 1, \ldots, 4$ are reference trajectories to be followed

$$
\begin{aligned}
r_1 &= q_T|_{t=T_{ss,start}} \times (1 - w_1) + q_{T,d} \times w_2 \\
r_2 &= (q_{st} + q_{sw})|_{t=T_{ss,start}} \times w_1 \\
r_3 &= L_{leg,nominal} \times (q_{st,d}|_{t=T_{ss,end}} - \text{sign}(q_{st}) \times q_{st})/k \\
r_4 &= L_{st,d}(q_{st}).
\end{aligned}
\tag{11}
$$

Tracing the reference trajectories r_1 and r_2 ensures a constant angle of the torso with respect to the vertical, say $q_{T,d}$, and forward advancement of the swing leg as mirror image of the stance leg. w_1 and w_2 are appropriately chosen exponential functions with time constant sufficiently smaller than the time duration of a single support. This ensures that the reference trajectories r_1 and r_2 converge in a smooth exponential manner from initial values at the start of the single support phase toward desired values. Such a definition of r_2 implies that q_{st} is a monotonically increasing function during the single support phase: $q_{st} \in [q_{st}|_{t=T_{ss,start}}, q_{st,d}|_{t=T_{ss,end}}]$.

The legs are assumed telescopic and its length moves around nominal leg length $L_{leg,nominal}$. Telescopic movement of the swing leg is determined to assure sufficient swing leg clearance and is set by constant k, which is proportional to $L_{leg,nominal}$ and in the range of normal human foot clearance. Tracing the reference trajectory r_3 ensures the tip of the swing leg to move away from the ground until the stance leg passes the vertical and to approach the ground afterward until $q_{st} = q_{st,d}|_{t=T_{ss,end}}$. It is assumed that when $q_{st} = q_{st,d}|_{t=T_{ss,end}}$, the tip of the swing leg touches the ground and the single support phase terminates. $q_{st,d}|_{t=T_{ss,end}}$ is related to the desired cadence $\text{cad}_{gait,d}$, the desired gait velocity $v_{gait,d}$, and the

desired step-length $L_{step,d}$. These parameters are defined as

$$
\begin{aligned}
L_{step,d} &= \frac{2v_{gait,d}}{\text{cad}_{gait,d}} = d_1 + d_2 \\
d_1 &= x_{st}|_{t=T_{ss,start}} - x_{sw}|_{t=T_{ss,start}} \\
d_2 &= 2L_{leg,nominal} \sin\left(q_{st,d}|_{t=T_{ss,end}}\right).
\end{aligned}
\tag{12}
$$

Lengthening and shortening as governed by reference trajectory r_4 determines a telescopic movement of the stance leg. It is defined as a fifth-order polynomial of q_{st} such that (see Fig. 2 for a representation)

$$
\begin{aligned}
L_{st}(q_{st} = q_{st}|_{t=T_{ss,start}}) &= L_{st}|_{t=T_{ss,start}} \\
\dot{L}_{st}(q_{st} = q_{st}|_{t=T_{ss,start}}) &= \dot{L}_{st}|_{t=T_{ss,start}} \\
L_{st}\left(q_{st} = \frac{q_{st}|_{t=T_{ss,start}} + q_{st,d}|_{t=T_{ss,end}}}{2}\right) &= L_{leg,nominal} \\
L_{st}\left(q_{st} = q_{st,d}|_{t=T_{ss,end}}\right) &= L_{leg,nominal} \\
\dot{L}_{st}\left(q_{st} = q_{st}|_{t=T_{ss,end}}\right) &= \dot{L}_{st,d}|_{t=T_{ss,end}}
\end{aligned}
\tag{13}
$$

where $\dot{L}_{st,d}|_{t=T_{ss,end}}$ is the desired stance leg extension velocity at the end of single support and is determined on higher between-step control level to assure constant gait velocity.

The output vector reads as

$$
y_{ss} = h_{ss}(q) = \begin{bmatrix} q_T - r_1 \\ q_{st} + q_{sw} - r_2 \\ z_{sw} - r_3 \\ L_{st} - r_4 \end{bmatrix}.
\tag{14}
$$

3.1.2. Within-step control in double support phase. The control strategy in the double support phase is composed of feedback control for the torso position, thus calculating the hip torques, and forward dynamics by directly applying the forces to the legs.

Evolution of feedback control in the double support phase is closely related to feedback control in the single support phase. We will continue controlling the torso angle yet suspend the mirrored-like behavior of stance and swing leg, as such an objective is in contradiction with the concept of double support. Namely, as both legs remain in contact with the ground throughout the double support phase, an increasing asymmetry between both legs is a natural evolution of biped walking if the horizontal position of the hip is to monotonically increase. Therefore, to assure invertibility of the decoupling matrix, the objective to control the torso angle will be encoded as

$$
\begin{aligned}
y_1 &= q_T - r_1 \\
y_2 &= q_T + \eta q_{sw} - r_2
\end{aligned}
\tag{15}
$$

where

$$
\begin{aligned}
r_1 &= q_T|_{t=T_{ds,start}} \times (1 - w_1) + q_{T,d} \times w_2 \\
r_2 &= (q_T|_{t=T_{ds,start}} + \eta q_{sw}|_{t=T_{ds,start}}) \\
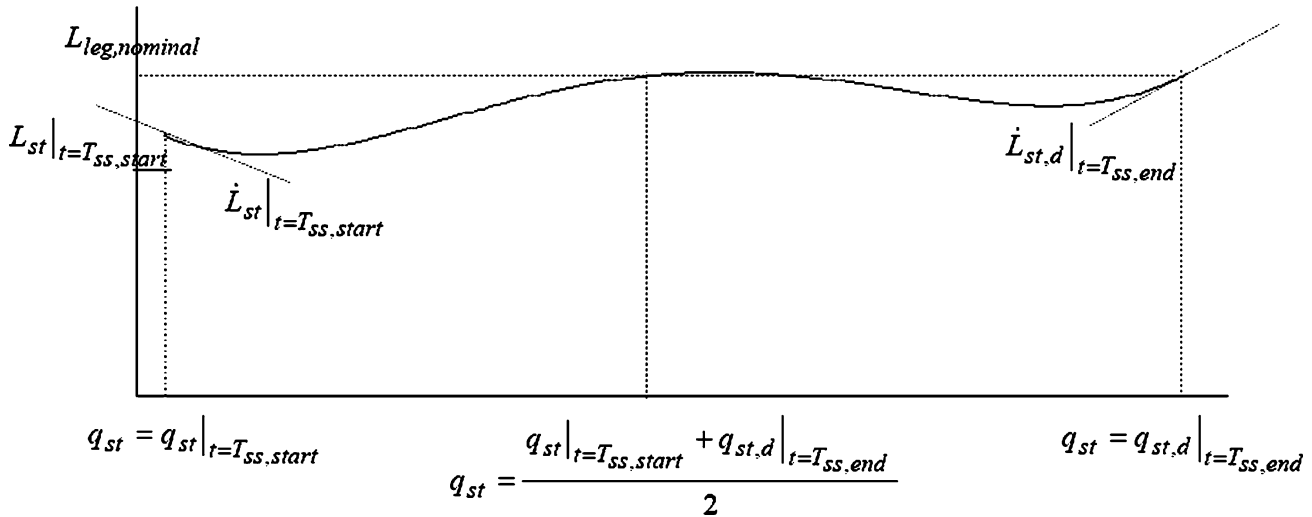&\quad \times (1 - w_1) + q_{T,d} \times w_2
\end{aligned}
\tag{16}
$$

Fig. 2. Fifth-order polynomial representing reference trajectory $r_4 = L_{st,d}(q_{st})$.

and choosing the constant $\eta \ll 1$ avoids singularity of the decoupling matrix. w_1 and w_2 are appropriately chosen exponential functions with time constant sufficiently smaller than the time interval of a double support. This ensures that the reference trajectories r_1 and r_2 converge in a smooth exponential manner from initial values at the start of the double-support phase toward desired values.

The output vector reads as

$$y_{ds} = h_{ds}(q) = \begin{bmatrix} q_T - r_1 \\ q_T + \eta q_{sw} - r_2 \end{bmatrix}. \tag{17}$$

Forward dynamics assumes exponentially increasing F_{sw} and appropriately chosen parabolic function for decreasing F_{st} from $F_{st}|_{t=T_{ss,end}}$. The double support phase is considered terminated when F_{st} reaches zero value

$$F_{st}|_{t=T_{ds,end}} = 0. \tag{18}$$

3.1.3. Controller design. The control objective is to drive the outputs of single and double support, $y_{ss} = h_{ss}(q)$ and $y_{ds} = h_{ds}(q)$, respectively, to zero. Since the outputs only depend on configuration variables and the dynamic model is of second order, the relative degree of the output is two. Following the standard Lie derivative notation,[30] direct calculation yields

$$\ddot{y} = L_f^2 h(q, \dot{q}) + L_g L_f h(q) u \tag{19}$$

and the overall feedback applied is given by

$$u = -(L_g L_f h)^{-1} (L_f^2 h + K_D L_f h + K_P h) \tag{20}$$

where $L_g L_f h(q)$ is the decoupling matrix and is assumed invertible and K_D and K_P are positive-definite gain matrices. We refer to Isidori[29] for a detailed overview of feedback control.

The internal dynamics of the system when the outputs $y_{ss}(q)$ and $y_{ds}(q)$ are identically zero is referred to as the zero

dynamics. Thus,

$$\begin{aligned} Z_{ss} &= \{(q', \dot{q}') \in TQ | h_{ss}(q) = 0, L_f h_{ss}(q) = 0\} \\ Z_{ds} &= \{(q', \dot{q}') \in TQ | h_{ds}(q) = 0, L_f h_{ds}(q) = 0\} \end{aligned} \tag{21}$$

denote zero dynamics of single and double support, respectively.

3.2. Between-step control
Between-step control introduces adaptive variation of the desired stance leg lengthening velocity at the end of the single support phase $\dot{L}_{st,d}|_{t=T_{ss,end}}$ in a sense that greater $\dot{L}_{st,d}|_{t=T_{ss,end}}$ necessitates greater $F_{st}|_{t=T_{ss,end}}$, whereas greater $F_{st}|_{t=T_{ss,end}}$ implies more pronounced push-off and vice versa. Such a control strategy allows us to influence forward propulsion to assure constant gait velocity. In a condensed form, between-step control can be expressed as

$$\begin{aligned} \dot{L}_{st,d}^k\big|_{t=T_{ss,end}} &= \dot{L}_{st,d}^{k-1}\big|_{t=T_{ss,end}} + k_p\big(v_{gait}^{k-1} - v_{gait,d}\big) \\ &\quad + k_d\big(v_{gait}^{k-1} - v_{gait}^{k-2}\big) \end{aligned} \tag{22}$$

where the superscript k indicates the gait-cycle number, k_d and k_p are positive gains and

$$v_{gait}^k = \frac{x_H^k\big|_{t=T_{ds,end}} - x_H^k\big|_{t=T_{ss,start}}}{T_{ds,end} - T_{ss,start}}. \tag{23}$$

Such a definition of between-step control implies adaptation of $h_{ss}(q)$ after each step in a sense to find stance leg lengthening/shortening, which would lead to the desired gait velocity. Furthermore, this makes single support zero dynamics time variant

$$\begin{aligned} Z_{ss} = Z_{ss}(k) = \{(q', \dot{q}') \in TQ | h_{ss}(q, k) \\ = 0, L_f h_{ss}(q, k) = 0\} \end{aligned} \tag{24}$$

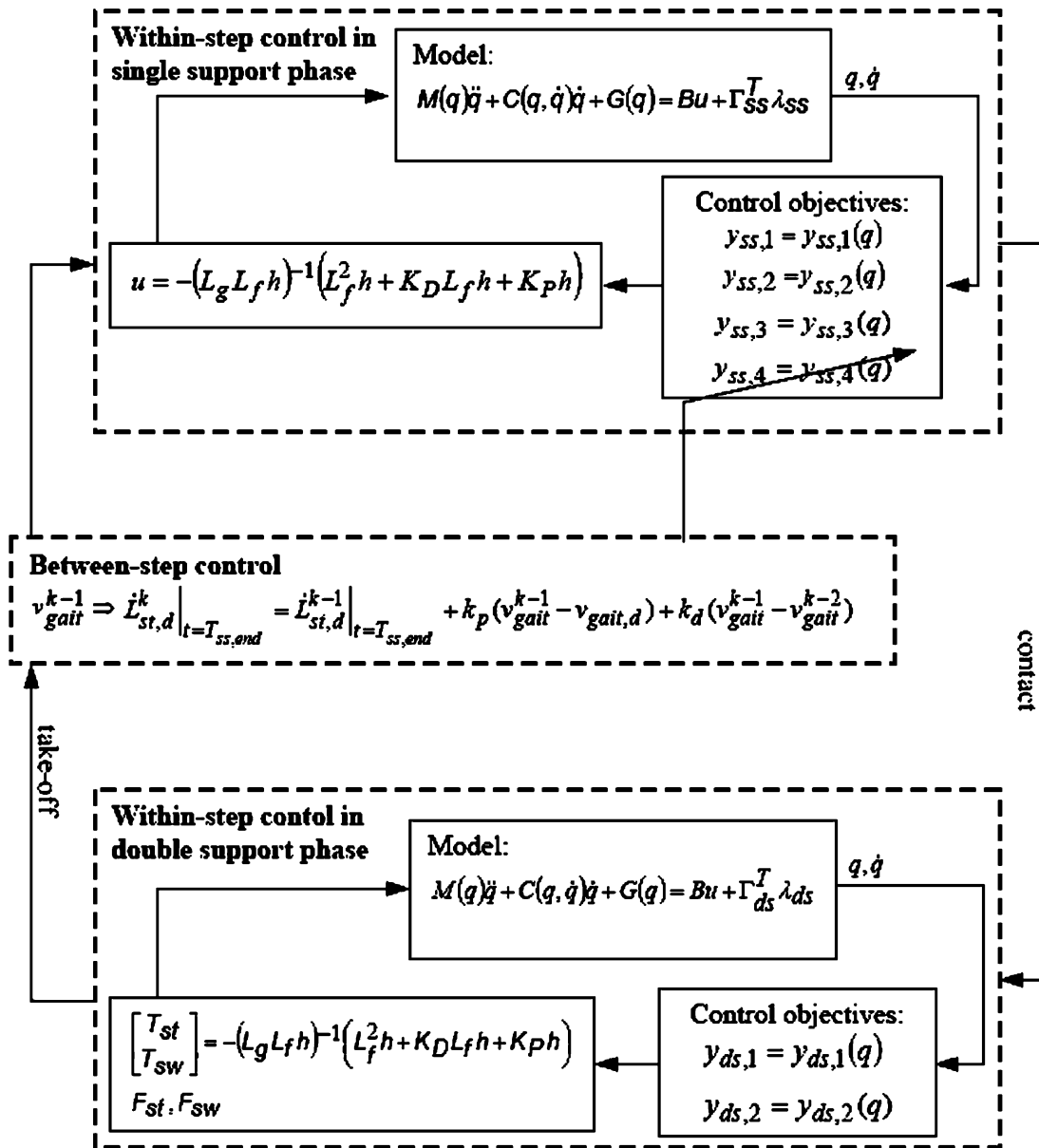The overall control strategy is illustrated in Fig. 3.

Fig. 3. Schematic representation of the overall control strategy.

4. Simulation Cases

Eight simulation cases, as listed in Table I, were selected to test the performance and stability of the proposed control strategy. A high diversity between simulation cases (Cases 1–8) was selected to investigate the performance of the control strategy in a wide range of walking modes. We further investigated how power absorption and push-off accommodate to account for changes in gait velocity (Cases 3–6) and torso angle (Cases 7–8) and how our findings relate to human walking, where greater gait velocity is accompanied with an increase in power absorption and push-off whereas the anteriorly inclined torso shifts the center of mass forward, which contributes significantly to forward progression and downward fall leading to more

Table I. Simulation cases: Desired kinematics and model parameters.

		Case 1	Case 2	Case 3	Case 4	Case 5	Case 6	Case 7	Case 8
$v_{\text{gait,d}}$	m/s	0.60	0.70	0.80	0.90	1.00	1.10	1.10	1.10
$L_{\text{step,d}}$	m	1.20	1.20	0.96	1.08	1.20	1.32	1.32	1.32
$q_{\text{T,d}}$	rad	0	0	0	0	0	0	0.1	0.20
$\text{cad}_{\text{gait,d}}$	steps/min	60	70	100	100	100	100	100	100

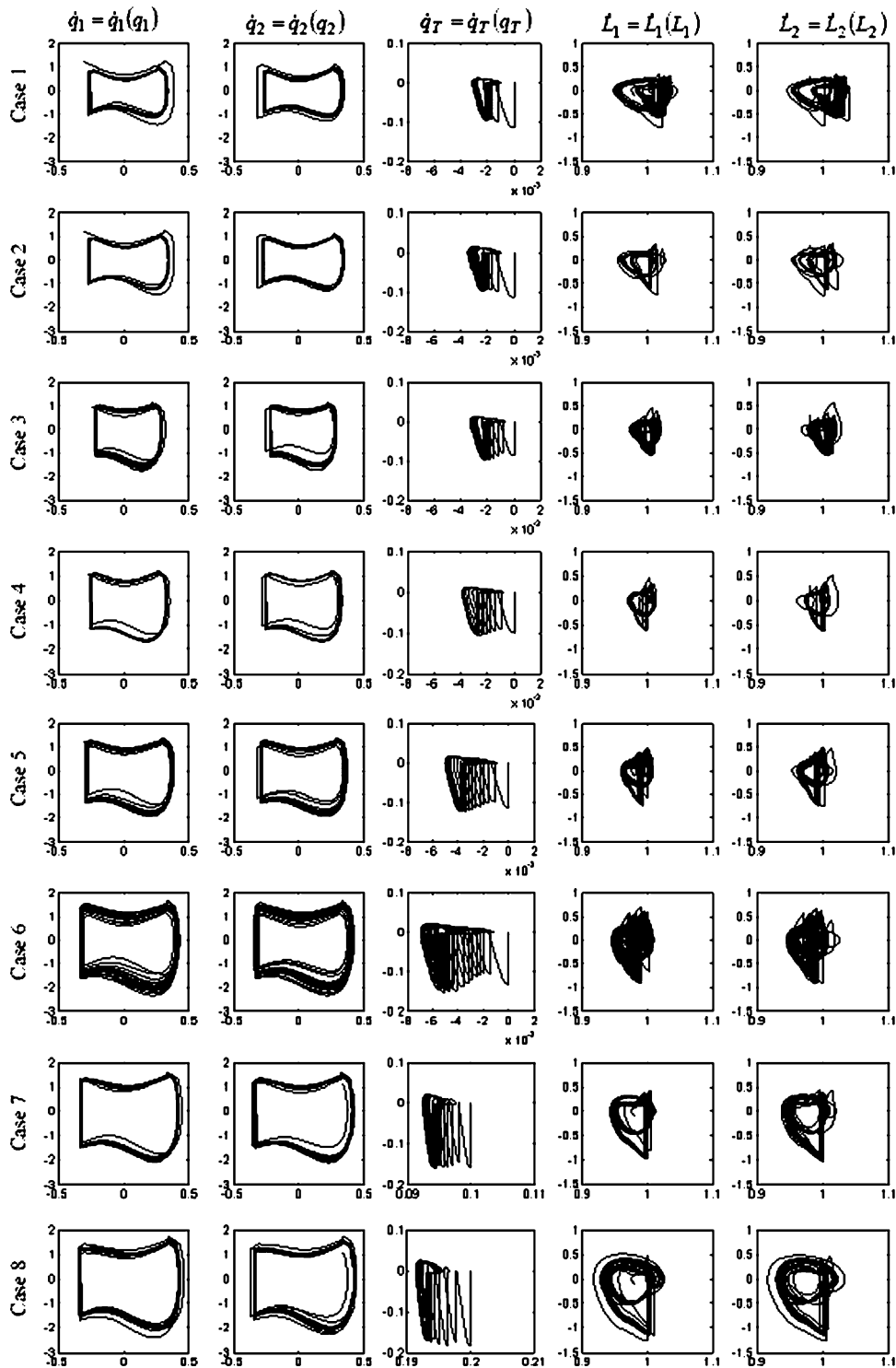| $m_L = 10\,\text{kg}$	$m_H = 10\,\text{kg}$	$m_T = 40\,\text{kg}$	$I_L = 1.75\,\text{kgm}^2$	$I_T = 3.50\,\text{kgm}^2$
$L_T = 0.40\,\text{m}$	$L_{\text{leg,nominal}} = 1\,\text{m}$			

Fig. 4. State space orbits for all simulation cases. Each orbit is parameterized with respect to configuration variable (horizontal axis) and its derivative (vertical axis). State space orbits in one column relate to the same configuration variable. State space orbits in one row refer to the same simulation case.

pronounced power absorption and less pronounced push-off. In a period of one cycle, we focused on the first peak in vertical ground reaction forces as an indication of power absorption and on second peak as an indication of push-off. $K_{D,ss}$, $K_{P,ss}$, $K_{D,ds}$, $K_{D,ds}$, k_p, and k_d were experimentally determined and remained unchanged in all simulation cases.

We used the MATLAB software and the MATLAB Simulink toolbox to obtain a mathematical model of the

biped walker and to perform simulations, respectively. It took approximately 15 min on a personal computer (Intel Pentium 4, 2.4 GHz, 2.0-GB RAM) to complete 60 gait cycles in each simulation case.

5. Results
Figure 4 displays a set of state space orbits for each simulation case. Each simulation case displays stable walking as only
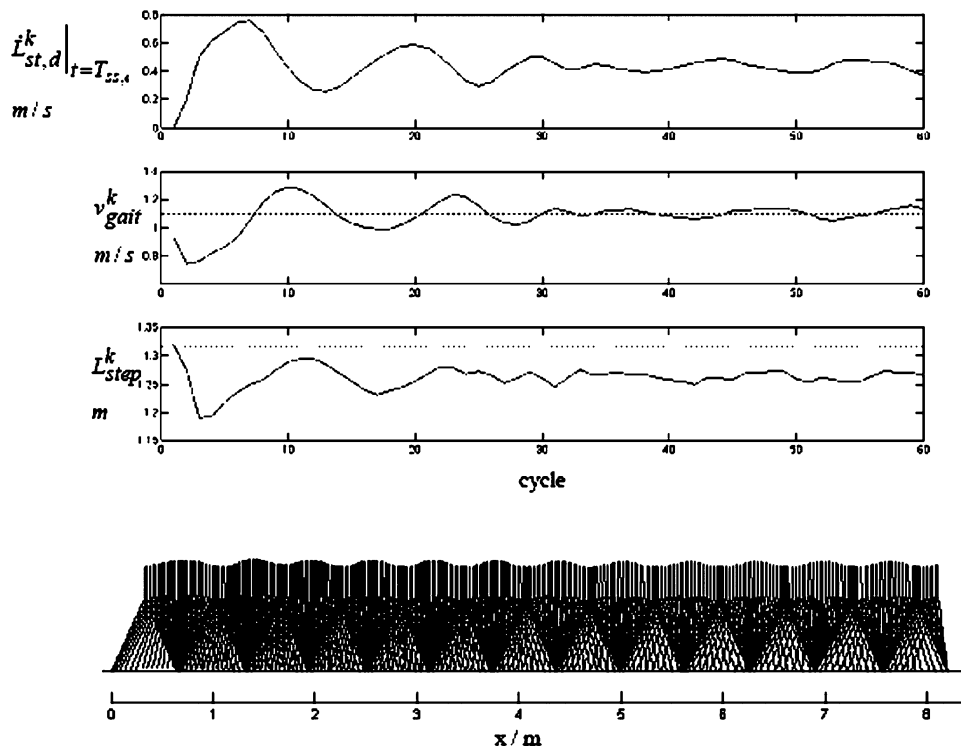
Fig. 5. Case 6: Controller's performance in the first 60 walking cycles and a stick diagram visualizing walking of the model.

a few initial steps are necessary for the robot to settle in a stable state space orbit. In this respect, we consider Case 6, by far the most extreme example, as somewhat more dispersed orbits indicate more steps being needed for a stable cyclic walking. This is also evident in Fig. 5, which demonstrates the performance of between-step control. We notice considerable discrepancy between v_{gait}^k and $v_{\text{gait,d}}$ as well as L_{step}^k and $L_{\text{step,d}}$ in the first few steps until the adaptive control of $\dot{L}_{\text{st,d}}|_{t=T_{\text{ss,end}}}$ takes effect leading to a gradual convergence to a stable walking at desired gait velocity and somewhat shorter step length than desired afterwards.

The effect of $\dot{L}_{\text{st,d}}|_{t=T_{\text{ss,end}}}$ between-step control is also evident in hip torques and leg forces (Fig. 6) as well as in ground reaction forces (Fig. 7). The control system responds to an $\dot{L}_{\text{st,d}}|_{t=T_{\text{ss,end}}}$ increase by increasing hip torques and stance leg force at the end of the single support phase, which leads to greater horizontal and vertical ground reaction forces indicating more pronounced push-off. When comparing the cycle duration, we notice that greater push-off is followed by a shorter cycle duration.

Figure 8a shows that pronounced push-off, as indicated by the second peak in vertical ground reaction force, as well as power absorption, as indicated by the second peak in vertical ground reaction force, are necessary if walking is to be faster. On the other hand, when the torso is inclined anteriorly, more power absorption and less pronounced push-off are needed to maintain constant gait velocity, while hip actuators have to generate more torque during the single support phase (Fig. 8b).

We also tested how well the model can adapt to a gait velocity change while walking. Figure 9 shows the performance of the model when the desired gait velocity is increased successively in steps of 0.1 m/s from 0.8 to 1.1 m/s. Note that the controller followed the desired changes in gait velocity indicating its feasibility in a wide range of walking regimes.

6. Stability Analysis

Time-variant zero dynamics that results from between-step control of stance leg lengthening velocity means that the system's states cannot be expressed as a time-invariant function of a single selected state, which would enable development of explicit, low-dimensional tests of stability properties of the system that are based on a reduced one-dimensional Poincaré return map.[5, 28]

Therefore, the stability of a developed biped walking model can only be evaluated in simulations by analyzing a complete Poincaré return map of the system. For an n-dimensional dynamic system (2), a Poincaré section S is defined as an $n-1$ dimensional surface that the system crosses exactly once during each period and the return map is a mapping from one intersection to the next

$$x_{n+1} = r(x_n). \tag{25}$$

We quantified the stability of the biped walking model by experimentally examining the eigenvalues of the linearized return map through the hyperplane $q_{\text{st}} = 0$, $\dot{q}_{\text{st}} > 0$ in eight simulation cases as defined in Table I. For each trial, we created a set of vectors x_i, which represent the state of the system on the ith crossing, and estimated the fixed point x_{f} as the average of the last five crossings, assuming the model has settled in stable gait. Finally we performed a least-square
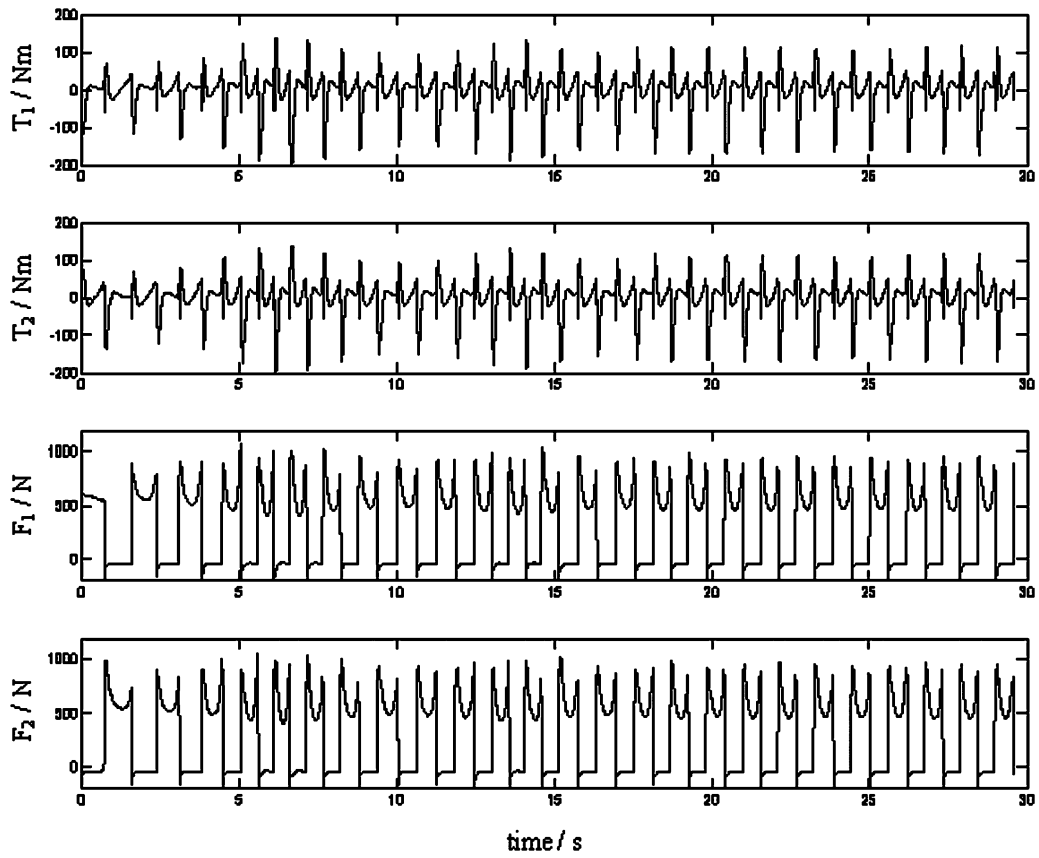
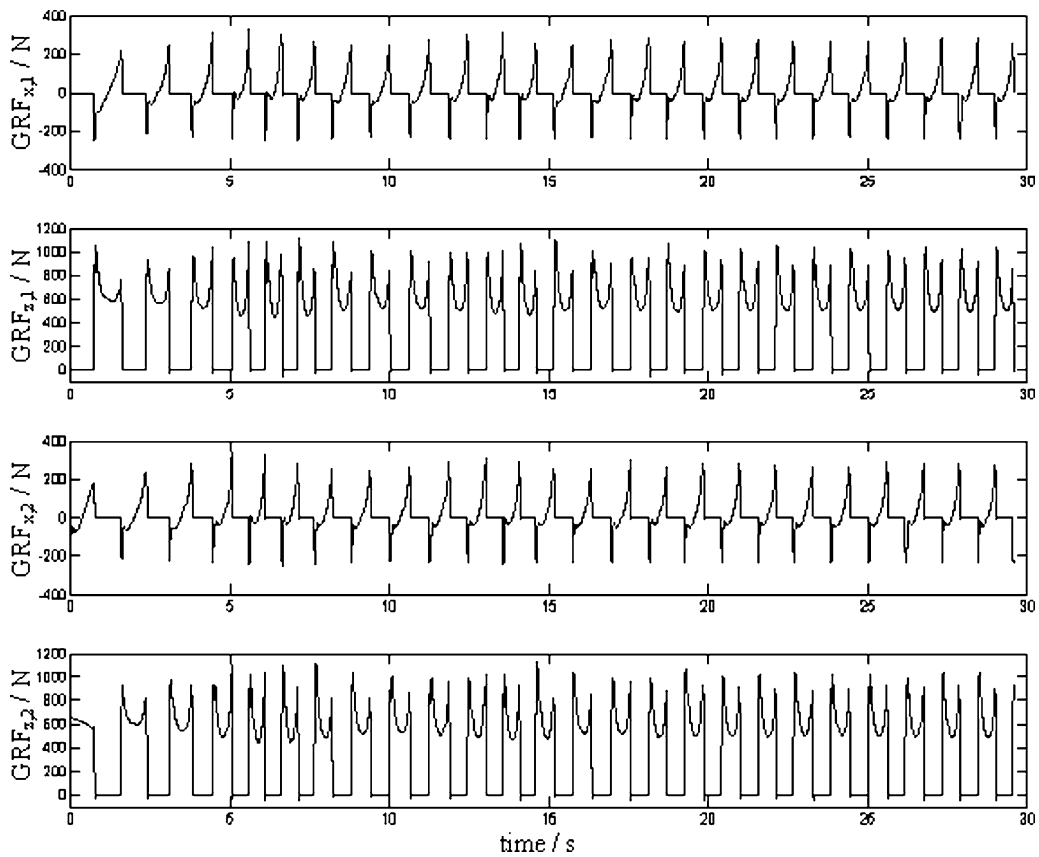Fig. 6. Case 6: Hip torques and leg forces in the first 50 walking cycles.

Fig. 7. Case 6: Horizontal and vertical ground reaction forces in the first 50 walking cycles. In a period of one cycle, the first and second peak in vertical ground reaction forces indicate power absorption and push-off, respectively.
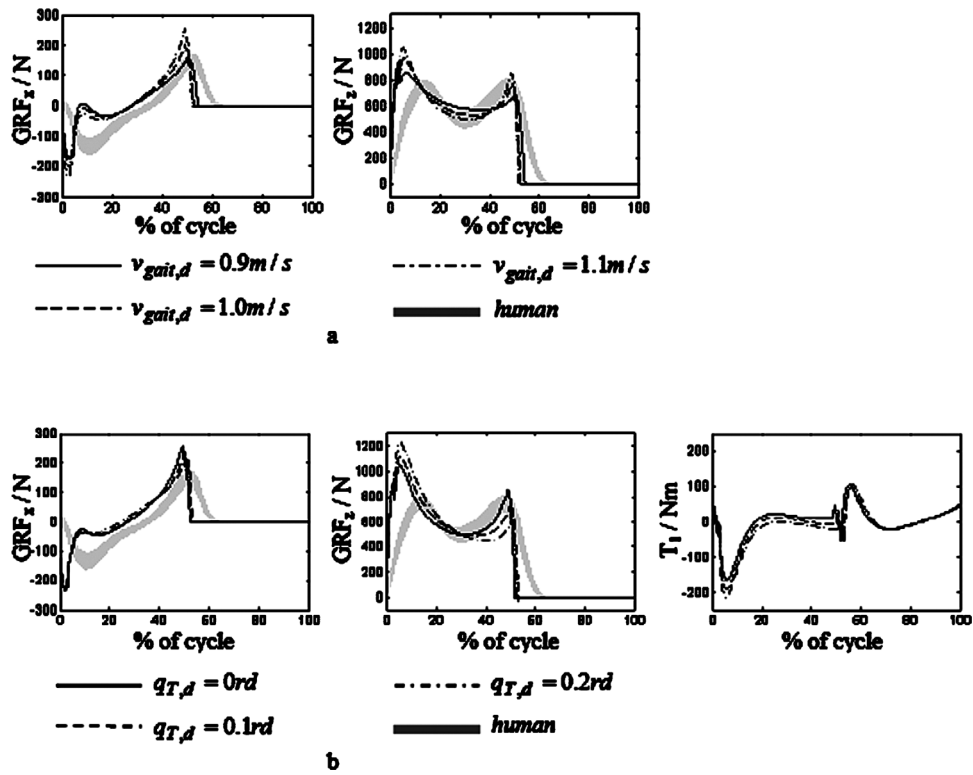
Fig. 8. (a) Relation between gait velocity and power absorption and push-off (b) and relation between torso position and power absorption and push-off. For comparison, the average human ground reaction forces are shown (adopted from Winter *et al.*[20])
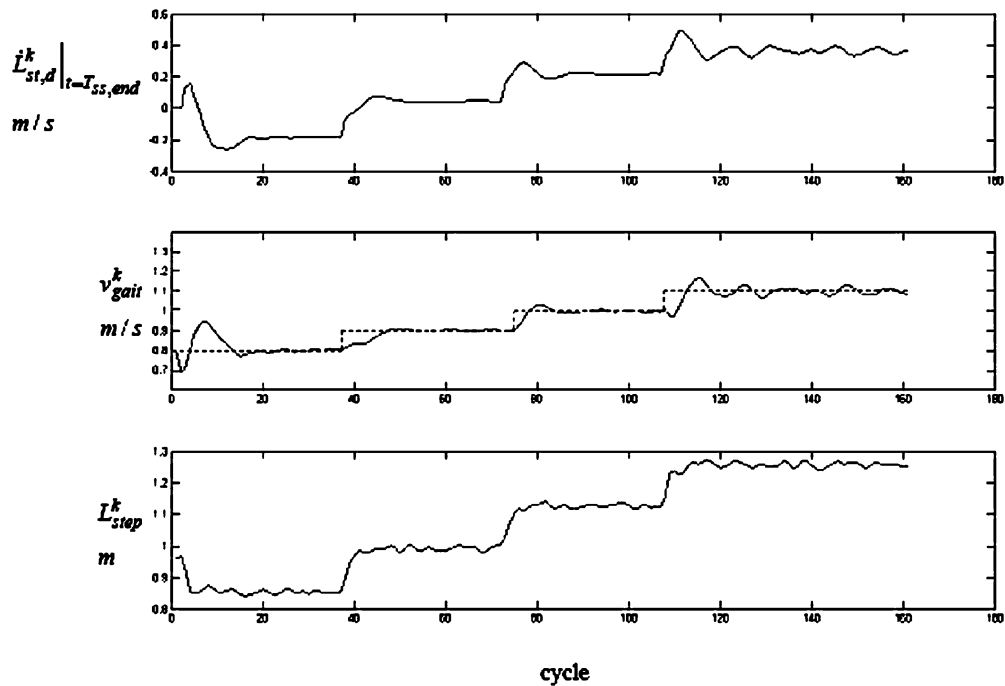

Fig. 9. Increasing desired gait velocity while walking in successive steps of 0.1 m/s from 0.8 to 1.1 m/s.

Table II. Stability analysis.

	Case 1	Case 2	Case 3	Case 4	Case 5	Case 6	Case 7	Case 8
Maximal eigenvalue	0.92	0.64	0.76	0.84	0.78	0.79	0.74	0.72

fit of the matrix A to satisfy

$$(x_{i+1} - x_f) = A(x_i - x_f) \qquad (26)$$

The matrix A can, then, be expressed as

$$A = YX^T(XX^T)^{-1} \qquad (27)$$

where

$$\begin{aligned} X &= [x_1 - x_f, x_2 - x_f \ldots x_{n-1} - x_f] \\ Y &= [x_2 - x_f, x_3 - x_f \ldots x_n - x_f] \end{aligned} \qquad (28)$$

and the eigenvalues of A are calculated. Maximal eigenvalues for eight simulation cases are listed in Table II. All eigenvalues are less than one indicating local stability in all examined cases.

7. Conclusion

The main contribution of this paper is the introduction of between-step control in a way that enables adaptive control of gait velocity with the same set of controller's gains. In contrast to similar bipedal models, where the kinematically based trajectory tracking has been predominantly used, we placed the proposed two-level control strategy within the kinetic framework. The robot's gait may ultimately be controlled through kinematics; however, the desired kinematics is governed by the desired kinetics. The relation between the kinematics and kinetics is determined on between-step control level by setting the desired stance leg lengthening velocity at the end of the single support phase to achieve appropriate push-off for gait velocity control. The proposed control strategy has proven to be feasible and can generate human-like behavior in push-off and power absorption pattern to account for the desired gait velocity and torso position variations in a way similar to that seen in human walking, where higher gait velocity necessitates more pronounced push-off at the end of stance phase and greater power absorption during the double support phase. Also, consistent with the observations of human walking, increased forward trunk inclination decreased the push-off and increased power absorption at the same gait velocity.

Even though the model used in our study is simple, it can be extended to have also the knees and ankles instead of telescopic legs. By doing so, legs will have two actuators and optimization criteria will be needed to determine relative contribution of the knee and ankle actuators. Such an optimization can be set up by applying the proposed control strategy in a way to govern the desired kinetics while controlling the desired virtual leg length (line connecting the hip and the contact point). This will enable us to even further match kinematics and kinetics of biped walking machines with those in humans.

References

1. F. E. Zajac, R. R. Neptune and S. A. Kautz, "Biomechanics and muscle coordination of human walking Part I: Introduction to concepts, power transfer, dynamics and simulations," *Gait Posture* **16**, 215–232 (2002).
2. F. E. Zajac, R. R. Neptune and S. A. Kautz, "Biomechanics and muscle coordination of human walking Part II: Lessons from dynamical simulations and clinical implications," *Gait Posture* **17**, 1–17 (2003).
3. J. W. Grizzle, C. H. Moog and C. Chevallereau, "Nonlinear control of mechanical systems with an unactuated cyclic variable," *IEEE Trans. Autom. Control* **30**(5), 559–576 (2005).
4. E. R. Westervelt, J. W. Grizzle and D. E. Koditschek, "Hybrid zero dynamics of planar biped walkers," *IEEE Trans. Autom. Control* **48**(1), 42–56 (2003).
5. J. W. Grizzle, G. Abba and F. Plestan, "Asymptotically stable walking for biped robots: Analysis via systems with impulse effects," *IEEE Trans. Autom. Control* **46**(1), 51–64 (2001).
6. F. Plestan, J. W. Grizzle, E. Westervelt and G. Abba, "Stable walking of a 7-DOF biped robot," *IEEE Trans. Robot. Autom.* **19**(4), 653–668 (2003).
7. F. C. Anderson and M. G. Pandy, "Dynamic optimization of human walking," *J. Biomech. Eng.* **231**, 381–390 (2001).
8. L. A. Gilchrist and D. A. Winter, "A multisegment computer simulation of normal human gait," *IEEE Trans. Rehabil. Eng.* **5**(4), 290–299 (1997).
9. M. W. Spong and F. Bullo, "Controlled symmetries and passive walking," *IEEE Trans. Autom. Control* **50**(7), 1025–1031 (2005).
10. X. Mu and Q. Wu, "Synthesis of a complete sagittal gait cycle for a five-link biped robot," *Robotica* **21**, 581–587 (2003).
11. R. Q. van der Linde, "Design, analysis, and control of a low power joint for walking robots, by phasic activation of McKibben muscles," *IEEE Trans. Robot. Autom.* **15**(4), 595–604 (1999).
12. T. McGeer, "Passive dynamic walking," *Int. J. Robot. Res.* **8**(2), 68–83 (1990).
13. T. McGeer, "Passive Walking With Knees," *Proceedings of the 1990 IEEE Robotics and Automation Conference*, Cincinnati, OH (May 1990) pp. 1640–1645.
14. R. Q. van der Linde, "Passive bipedal walking with phasic muscle contraction," *Biol. Cybern.* **81**, 227–237 (1999).
15. H. Lim and A. Takanishi, "Compensatory motion for a biped walking robot," *Robotica* **23**, 1–11 (2005).
16. C.-L. Shih, "Gait synthesis for a biped robot," *Robotica* **15**, 599–607 (1997).
17. S. Collins, A. Ruina, R. Tedrake and M. Wisse, "Efficient bipedal robots based on passive dynamic walkers," *Sci. Mag.* **307**, 1082–1085 (2005).
18. M. Wisse, A. L. Schwab and F. C. T. van der Helm, "Passive dynamic walking model with upper body," *Robotica* **22**, 681–688 (2004).
19. S. Mochon and T. A. McMahon, "Ballistic walking," *J. Biomech.* **13**, 49–57 (1980).
20. E. R. Westervelt and J. W. Grizzle, "Design of Asymptotically Stable Walking for a 5-Link Planar Biped Walker via Optimization," *Proceedings of the IEEE International Conference on Robotics and Automation*, Washington, DC (2002) pp. 3117–3122.
21. L. Roussel, C. Canudas-de-Wit and A. Goswami, "Generation of Energy Optimal Complete Gait Cycles for Biped Robots," *Proceedings of the IEEE International Conference on Robotics and Automation*, Leuven, Belgium (1998) pp. 2035–2041.
22. M. Vukobratovic, A. A. Frank and D. JuriŁi, "On the stability of biped locomotion," *IEEE Trans. Biomed. Eng.* **17**(1), 25–36 (1970).
23. K. Mitobe, G. Capi and Y. Nasu, "Control of walking robots based on manipulation of the zero moment point," *Robotica* **18**, 651–657 (2000).
24. A. D. Kuo, "Energetics of actively powered locomotion using the simplest walking model," *J. Biomech. Eng.* **124**, 113–120 (2002).
25. D. A. Winter, "Biomechanical motor patterns in normal walking," *J. Motor Behav.* **15**, 302–330 (1983).

26. D. A. Winter, "Energy generation and absorption at the ankle and knee during fast, natural, and slow cadences," *Clin. Orthop. Relat. Res.* **175**, 147–154 (1983).
27. J. H. Choi and J. W. Grizzle, "Feedback control of an underactuated planar bipedal robot with impulsive foot action," *Robotica* **23**, 567–580 (2005).
28. S. Miossec and J. Aoustin, "A Simplified Stability Study for a Biped Walk With Under and Over Actuated Phases,"

Proceedings of the Robot Motion and Control Workshop, Poznan, Poland (2004) 53–59.
29. Y. Hurmuzlu and D. B. Marghitu, "Rigid body collisions of planar kinematic chains with multiple contact points," *Int. J. Robot. Res.* **13**(1), 82–92 (1994).
30. A. Isidori, *Nonlinear Control Systems: An Introduction*, 2nd ed. (Springer-Verlag, Berlin, Germany, 1989).